



Systemically administered low-affinity HER2 CAR T cells mediate antitumor efficacy without toxicity

Tamer Basel Shabaneh ¹, Andrew R Stevens,¹ Sylvia M Stull,¹ Kristen R Shimp,² Brandon W Seaton,² Ekram A Gad,³ Carla A Jaeger-Ruckstuhl,¹ Sylvain Simon ¹, Amanda L Koehne,⁴ Jason P Price,⁵ James M Olson,⁵ Benjamin G Hoffstrom,⁶ David Jellyman,⁶ Stanley R Riddell¹

To cite: Shabaneh TB, Stevens AR, Stull SM, *et al.* Systemically administered low-affinity HER2 CAR T cells mediate antitumor efficacy without toxicity. *Journal for ImmunoTherapy of Cancer* 2024;**12**:e008566. doi:10.1136/jitc-2023-008566

► Additional supplemental material is published online only. To view, please visit the journal online (<https://doi.org/10.1136/jitc-2023-008566>).

Accepted 03 January 2024



© Author(s) (or their employer(s)) 2024. Re-use permitted under CC BY-NC. No commercial re-use. See rights and permissions. Published by BMJ.

For numbered affiliations see end of article.

Correspondence to
Dr Stanley R Riddell;
sriddell@fredhutch.org

ABSTRACT

Background The paucity of tumor-specific targets for chimeric antigen receptor (CAR) T-cell therapy of solid tumors necessitates careful preclinical evaluation of the therapeutic window for candidate antigens. Human epidermal growth factor receptor 2 (HER2) is an attractive candidate for CAR T-cell therapy in humans but has the potential for eliciting on-target off-tumor toxicity. We developed an immunocompetent tumor model of CAR T-cell therapy targeting murine HER2 (mHER2) and examined the effect of CAR affinity, T-cell dose, and lymphodepletion on safety and efficacy.

Methods Antibodies specific for mHER2 were generated, screened for affinity and specificity, tested for immunohistochemical staining of HER2 on normal tissues, and used for HER2-targeted CAR design. CAR candidates were evaluated for T-cell surface expression and the ability to induce T-cell proliferation, cytokine production, and cytotoxicity when transduced T cells were co-cultured with mHER2+ tumor cells in vitro. Safety and efficacy of various HER2 CARs was evaluated in two tumor models and normal non-tumor-bearing mice.

Results Mice express HER2 in the same epithelial tissues as humans, rendering these tissues vulnerable to recognition by systemically administered HER2 CAR T cells. CAR T cells designed with single-chain variable fragment (scFvs) that have high-affinity for HER2 infiltrated and caused toxicity to normal HER2-positive tissues but exhibited poor infiltration into tumors and antitumor activity. In contrast, CAR T cells designed with an scFv with low-affinity for HER2 infiltrated HER2-positive tumors and controlled tumor growth without toxicity. Toxicity mediated by high-affinity CAR T cells was independent of tumor burden and correlated with proliferation of CAR T cells post infusion.

Conclusions Our findings illustrate the disadvantage of high-affinity CARs for targets such as HER2 that are expressed on normal tissues. The use of low-affinity HER2 CARs can safely regress tumors identifying a potential path for therapy of solid tumors that exhibit high levels of HER2.

BACKGROUND

Chimeric antigen receptor T cell (CAR T) therapy targeting B cell-lineage molecules such as CD19 and B-cell maturation antigen

WHAT IS ALREADY KNOWN ON THIS TOPIC

⇒ Human epidermal growth factor receptor 2 (HER2) is being investigated as a target antigen of chimeric antigen receptor (CAR) T cells in solid cancers. However, HER2-directed CAR T cells have exhibited both on-target off-tumor toxicities and lackluster antitumor efficacy. Preclinical modeling of HER2-directed CAR T cells has been hindered by the lack of immunocompetent animal models that facilitate studying strategies to enable antitumor efficacy without CAR T-cell recognition of endogenous HER2 on normal tissues.

WHAT THIS STUDY ADDS

⇒ These studies demonstrate the utility of immunocompetent murine models for studying CAR T cell-mediated off tumor, on target toxicity. The studies reveal that optimal in vivo control of HER2+ tumors requires low-affinity interactions between the CAR and HER2 and that using high-affinity CAR T cells leads to infiltration of normal HER2+ tissue and elicits lethal on-target off-tumor toxicity.

HOW THIS STUDY MIGHT AFFECT RESEARCH, PRACTICE OR POLICY

⇒ Our findings identify parameters (eg, CAR T-cell dose, lymphodepletion intensity, and CAR affinity) that must be considered when designing or systemically administering CAR T-cell therapies for targets expressed on normal tissues.

is effective in patients with refractory B-cell malignancies and multiple myeloma.^{1–3} On-target off-tumor (OTOT) elimination of normal B cells and plasma cells by CAR T is profound, but usually transient and manageable.⁴ Extending therapy with CAR T to solid tumors is hampered by a more immunosuppressive tumor microenvironment and heterogeneity in antigen expression. Furthermore, candidate targets are frequently

expressed on both cancerous and some vital normal cells, heightening the risk of OTOT toxicity.^{3,5}

Mitigating risk requires understanding the principles that govern toxicity. Unlike small molecules and therapeutic antibodies, the proliferation and biodistribution of CAR T complicates predicting the therapeutic window.^{6,7} Phase I clinical trials suggest a safety window exists for some CAR T targets in solid tumors while CAR T specific for other targets have caused severe toxicities. CAR T directed at epithelial growth factor receptor (EGFR) resulted in tolerable skin toxicities due to the epidermal expression of EGFR,^{8,9} while carbonic anhydrase IX-directed CAR T caused severe liver toxicity, requiring clinical trial termination.¹⁰ Trials targeting carcinoembryonic antigen-related cell adhesion molecule 5 showed a mixed safety profile, with some trials reporting no toxicity,^{11,12} while others reporting lung toxicity.¹³ Lethal toxicity in patients treated with mesothelin (MSLN)-directed CAR T was attributed to upregulation of MSLN under inflammatory conditions in normal lung tissue.¹⁴ Even for an individual antigen, differences in target epitope, CAR design and affinity, conditioning regimen and cytokine support, tumor type and location, and CAR T dose makes it difficult to determine safety.^{15,16}

Human epidermal growth factor receptor 2 (HER2) is a highly actionable cancer target. Although expressed on normal epithelial tissues and cardiomyocytes,^{17,18} HER2 is overexpressed in several epithelial cancers where it drives oncogenic signaling. Therapy with the monoclonal antibody trastuzumab or trastuzumab-based antibody drug conjugates has an acceptable safety profile in breast, gastric, and colorectal cancers and constitutes a standard-of-care.^{19–22} The success and relative safety of these HER2 antibodies spawned interest in developing HER2 CAR T therapy and more than 10 clinical trials (www.clinicaltrials.gov) are investigating HER2 CAR T. Anecdotal reports employing CARs derived from clinical HER2 antibodies generated discrepant results. One patient developed fatal acute respiratory failure after lymphodepleting chemotherapy, infusion of a high dose of HER2 CAR T designed with the trastuzumab single-chain variable fragment (scFv), and high-dose interleukin (IL)-2.²³ Other trials administered a lower dose of HER2-specific CAR T designed from non-trastuzumab scFvs after no or low-intensity lymphodepletion and without cytokine support, and did not observe toxicity, although antitumor activity was limited.^{24–26}

The development of HER2 CAR T therapies would benefit from a preclinical model to define parameters that correlate with safety and efficacy. Previous models expressed human HER2 (hHER2) in tumors or tissues of immunodeficient mice and had significant limitations. One strategy implanted xenogeneic tumors with varying levels of hHER2 expression at different sites, using CAR T recognition of the HER2-low tumors as surrogates for HER2-expressing normal tissue.²⁷ Alternative strategies used virally delivered hHER2 to drive ectopic expression on murine liver tissue²⁸ or germline hHER2 driven

by strong non-native promoters in immunocompetent mice.²⁹ However, these strategies employed unphysiologic expression levels and locations of HER2 that do not recapitulate the expression patterns in humans.

We speculated that HER2 targeted T-cell therapy might be informed by an immunocompetent animal model. We developed a monoclonal antibody specific for murine HER2 (mHER2) to determine the expression of mHER2 in tissues of C57BL/6J mice and found a remarkably similar pattern of expression to that described in humans.¹⁸ We generated a library of anti-mHER2 monoclonal antibodies with a range of affinities to construct CARs, facilitating analysis of the role of scFv affinity in antitumor efficacy and toxicity in mice receiving various CAR T doses and lymphodepletion regimens. Our studies show that low-affinity HER2 CAR T can be safely administered with lymphodepletion and eliminate tumor cells expressing high levels of HER2. Depending on the tumor model, antigen escape and acquired T-cell exhaustion were identified as barriers to durable efficacy. In contrast, high and moderate-affinity CAR T more effectively recognized antigen-low tumor cells in vitro but failed to enhance tumor control in vivo and were toxic to normal HER2-expressing tissues in mice that received prior lymphodepletion. Our findings identify parameters that determine OTOT toxicity for a target such as HER2 and illustrate the utility of immunocompetent models to design effective CAR T therapies for targets expressed on normal tissues.

METHODS

Cell lines

Truncated mHER2 (P70424 aa1-684) was synthesized using GeneArt (Thermo Fisher) and cloned into MSCVPuro (Addgene #68469) to transduce KP1233 cells (gift from Tyler Jacks) and generate KP^{mHER2}. Truncated mHER2 was cloned into lentiviral HIV7 to transduce B16F10 (ATCC CRL-6475) and generate B16F10^{mHER2}. To generate mHER2-KO variants of D2.OR (gift from Ann Chambers), mHER2-targeted sgRNAs were synthesized (Synthego) and complexed with Cas9 (Integrated DNA Technologies) for 15 min at 37°C. D2.OR cells were electroporated on the P3 Primary Cell 4D-Nucleofector (Lonza) and assessed for protein knockout by flow cytometry 1 week later.

Antibody discovery

Two female rats (IACUC PROTO202100025) were immunized and boosted at 3, 5, and 9 weeks with Complete Freund's Adjuvant (CFA; 50% by final volume) and 65 µg mHER2-hFc (Sino Biological #50714-M02H). Two rats were immunized with Adjuvax (Sigma Aldrich), mHER2.hFc (75 µg), and 3×10⁶ Kras^{G12D}/P53^{null} murine lung adenocarcinoma cells previously transduced with mHER2 (KP^{mHER2}). Serum reactivity to beads coated with mHER2 or to KP^{mHER2} was measured by flow cytometry, and three rats with the highest reactivity by mean

fluorescence intensity were euthanized on week 10 to generate hybridomas using electrofusion (BTX™) of splenocytes with Sp2/0 partner. Additional details on hybridoma and antibody characterization are in online supplemental material.

Immunohistochemistry

KP^{mHER2} tumors or cell pellets were fixed with buffered formalin (Fisher) for 24 hours at room temperature, transferred to 70% ethanol at 4°C and paraffin embedded. For staining normal murine tissue, organs were fixed with PAXgene (Qiagen) for 24 hours, transferred to Stabilizer (Qiagen) at 4°C, and paraffin embedded. Blocks were sectioned at 4 µm onto positively charged slides, baked for 30 min at 60°C, and dewaxed using the Prisma Plus (Tissue-Tek). Details on antigen retrieval and staining are provided in online supplemental material.

CAR constructs

Retroviral vectors (MP71) encoded the following sequences: CD8α signal peptide (P01731 aa1-27), myc tag (EQKLISEEDL), respective scFv with VH and VL chains separated by a GSTSGSGKPGSGEGSTKG linker, human IgG4 hinge,³⁰ murine CD28 transmembrane (P31041 aa151-177), murine CD28 (P31041 aa177-218) or 4-1BB (P20334 aa211-256), and CD3ζ (P24161 aa52-164), a P2A peptide, and truncated CD19 (P25918 aa1-321) or Thy1.1 (Q53Y×2 aa1-162). The variable region sequence of 7.16.4 was provided by André Lieber (University of Washington). Details on retroviral production are provided in online supplemental material.

T-cell transduction and adoptive transfer

CD8+T cells were negatively selected (Stem Cell) from spleen and lymph nodes of 6–8-week-old CD45.1 mice, and stimulated with 1 µg/mL plate-bound anti-CD3 (145–2C11) and anti-CD28 (37.51) for 18–20 hours at 37°C 5% CO₂ in complete Roswell Park Memorial Institute (RPMI) media (RPMI-1640, 10% heat-inactivated FBS, 1 mM HEPES, 100 U/mL penicillin/streptomycin, 1 mM sodium pyruvate, and 50 µM β-mercaptoethanol) supplemented with 50 U/mL human IL-2 (PeproTech). Retrovirus was captured for 2 hours at 2,560 rcf at 32°C onto wells pre-coated with RetroNectin (Takara) and CD8+T cells (1×10⁶ cells/mL) added in IL-2-containing complete RPMI and mouse T-activator Dynabeads (Thermo Fisher) at 1:1 ratio. Plates were centrifuged at 800 rcf for 30 min at 32°C and incubated overnight. T cells were resuspended in IL-2-containing media and incubated for an additional 72 hours. Activator beads were removed and transduction efficiency determined by flow cytometry. For infusion, CAR T cells were resuspended at the indicated number per 100 µL serum-free RPMI-1640. 6–8-week-old C57BL/6J female mice were preconditioned as indicated and 6 hours later injected intravenously with CAR T cells.

Flow cytometry

50 µL of peripheral blood was collected into EDTA-coated tubes, and surface staining was performed after two rounds of ammonium–chloride–potassium (ACK) lysis. Spleens were dissociated, filtered through 100 µm strainer, and lysed with ACK twice before staining. Tumors were digested using Miltenyi Mouse Tumor Dissociation Kit and filtered through 100 µm strainer before staining. Debris was removed from B16F10 and B16F10^{mHER2} tumors using 40%–80% discontinuous Percoll gradient. Single-cell suspensions were supplemented with counting beads and stained using Live/Dead Fixable Aqua Dead Cell stain (Invitrogen) at 4°C for 15 min and TruStain FcX antibody for 10 min. Blood-circulating CAR T were stained for 30 min in flow buffer (phosphate-buffered saline, 1 mM EDTA, 2% FBS). Antibodies used for staining T cells are provided in online supplemental methods. To assess mHER2 expression, 1×10⁵ D2.OR cells were stained with 2.5 µg/mL 1G3 antibody and anti-rat PE secondary antibody (poly4054). Alternately, mouse anti-rat HER2 (clone 7.16.4; Bio X Cell) was directly conjugated with PE using PE Lightning-Link kit (Abcam) and used at 10 µg/mL to stain 1×10⁵ D2.OR cells. To determine the EC₅₀ values of anti-mHER2 antibodies, threefold dilutions of ≤9 µg/mL protein-G-purified antibody was used to stain D2.OR cells followed by anti-rat PE. Data analysis was performed on FlowJo V.10 software (TreeStar).

In vitro assays

Duplicate co-cultures of 5×10⁴ CAR T and 2.5×10⁴ target tumor cells (irradiated with 100 Gy) were incubated for 24 hours, and supernatants were analyzed for interferon (IFN)-γ and IL-2 by ELISA (Invitrogen). When using plate-bound mHER2.Fc for CAR T activation, High-Bind wells (Corning 3361) were coated with 20 µg/mL rabbit anti-human IgG Fc antibody overnight at 4°C and blocked with 2% bovine serum albumin (BSA) for 30 min at room temperature (RT). mHER2.Fc at the indicated concentrations was captured for 4 hours at RT and 1×10⁵ CAR T cells were added and incubated at 37°C for 24 hours before supernatant harvest for IFN-γ analysis. Assays were read using Synergy H4 reader and Gene5 software (BioTek). For chromium release assay, target cells were labeled with ⁵¹Cr (PerkinElmer) overnight, washed and incubated in triplicate for 24 hours with effector T cells at the indicated effector-to-target (E:T) ratio. For fluorescence-based killing assays, 1×10⁴ target cells (GFP+D2.0R or NucLight Red+B16F10 or B16F10.mHER2) were plated in triplicates in 96-well plates. CAR T were added at 10:1, 3:1, 1:1 E:T ratios in complete RPMI. Real-time imaging of fluorescence intensity was performed on xCELLigence RTCA eSight (Agilent). For impedance-based cytotoxicity, D2.0R or mHER2^{KO} D2.0R cells were plated overnight on 96-well E-plates (Agilent) and impedance (cell index) was measured over time and normalized to 100% when effector cells were added at 10:1 E:T ratio. To assess CAR T-cell proliferation, 5×10⁴ T cells were labeled with 5 µM CellTrace Violet dye (Invitrogen) and incubated

in duplicates with irradiated 2.5×10^4 target cells. After 72 hours, cells were stained with anti-CD8 α FITC, L/D aqua, Thy1.1 APC and analyzed by Celesta 2 for cell division.

In vivo models

The Fred Hutch Cancer Center (FHCC) Institutional Animal Care and Use Committee (IACUC) approved all mouse experiments (PROTO000050884). C57BL/6J (CD45.2+) and B6.SJL-Ptprca Pepcb/BoyJ (CD45.1+) mice were acquired from Jackson Laboratory and housed at the FHCC. C57BL/6J female mice (6–8-week-old) were injected subcutaneously into the right flank with 2×10^5 (KP^{mHER2}), 1×10^5 (B16F10), or 4×10^5 (B16F10^{mHER2}) tumor cells, lymphodepleted on day 7 (KP^{mHER2}) or 10 (B16F10 and B16F10^{mHER2}), and injected with CAR T 6 hours later. Calipers were used to monitor tumor size, and volume was calculated in mm³ as $L \times W \times \text{hour}$. Humane endpoint criteria were met when mice exhibited 20% weight loss or severe disease by body score.

Blood serum analysis

Retroorbital blood was incubated in serum separator tubes at room temperature for 30 min to allow clotting and centrifuged for 5 min. Serum was submitted to Zoetis labs for chemistry analysis, or to the FHCC Immune Monitoring core for Luminex Assay (R&D Systems).

Statistics

Statistical differences were determined using analysis of variance with Šídák, Tukey, Bonferroni, or Dunnett post-tests as indicated. Mice were randomized when assigned to treatment groups. Statistical analyses were performed using Prism V.10 (GraphPad), and differences considered significant if $p \leq 0.05$.

RESULTS

Normal tissue expression of HER2 is similar in mice and humans

To determine whether immunocompetent mice could inform studying toxicities of HER2 CAR T, we assessed mHER2 expression on tissues from normal mice and those engrafted with Kras^{G12D}/P53^{null} (KP) murine lung cancer cells transduced with the transmembrane and ectodomains of mHER2 (KP^{mHER2}) or hHER2 (KP^{hHER2}). Because the ectodomains of mHER2 and hHER2 exhibit 86% identity in amino acid sequence (online supplemental figure 1A), we evaluated the rabbit antibody SP101 that is specific for the ectodomain of hHER2 for immunohistochemistry (IHC).³¹ SP101 stained cell pellets of KP^{mHER2} and KP^{hHER2}, an hHER2+ tumor section, and implanted KP^{mHER2} tumors (online supplemental figure 1B). However, strong SP101 staining of normal murine smooth muscle and non-epithelial lung tissue was inconsistent with the expected distribution of mHER2, suggesting SP101 cross-reacted with other murine proteins.¹⁸ CB11 and DAKO A0485 anti-HER2 antibodies

that recognize epitopes in the hHER2 endodomain did not stain KP^{mHER2} and exhibited inconsistent staining of murine lung and skin epithelium, which are expected to express mHER2 (online supplemental figure 1B).

To obtain antibodies specific for the mHER2 ectodomain (ECD) and suitable for both IHC and CAR design, we immunized rats with mHER2-expressing murine tumor cells and/or recombinant mHER2 ECD fused to human Fc (online supplemental figure 1C). We isolated a library of mHER2-specific antibodies that varied in binding affinity for mHER2 and cross-reactivity to hHER2 (online supplemental figure 1D–F). A high-affinity mHER2-specific clone (1G3) from this library stained D2.OR murine mammary tumor cells but not D2.OR in which mHER2 was deleted by gene editing (figure 1, A and B) and did not cross react with hHER2 (online supplemental table 1, online supplemental figure 2). 1G3 was evaluated for IHC of subcutaneously implanted KP^{mHER2} and normal tissues. We identified uniform staining of KP^{mHER2} but not neighboring normal tissue, and staining of epithelium of the gastrointestinal tract villi, esophagus, bile ducts, endometrium, epidermis, and bronchi but not alveoli or smooth muscle (figure 1C,D, online supplemental figure 2). Staining with 1G3 was similar to the expression patterns observed when staining with the anti-HER2 antibody A0485 but without the presumed cross-reactive staining in lymph node and bone marrow observed with A0485 (online supplemental figure 2). The normal tissues that expressed mHER2 expression recapitulated the patterns of hHER2 in human tissues,^{18 32 33} supporting the use of the murine model for studying potential toxicities and antitumor activity of HER2-directed CAR T.

Low-affinity mHER2 CAR T cells eliminate HER2-high tumor cells and spare normal HER2+ tissues

We next examined whether mHER2 CAR T could be safely transferred to mice bearing syngeneic mHER2+ tumors. Given the expression of mHER2 on normal epithelium, we first tested a CAR constructed with a low-affinity scFv from the anti-rat HER2 antibody 7.16.4.³⁴ Although specific for rat HER2, 7.16.4 cross-reacted with mHER2 as shown by staining of KP^{mHER2} but not KP parental tumor cells (figure 2A). CARs derived from 7.16.4 were designed with an N-terminal myc tag on the scFv, a short IgG4 spacer, CD28 transmembrane domain, either CD28 or 4-1BB linked to CD3 ζ , and a truncated murine CD19 transduction marker (figure 2B). Murine T cells expressing the 7.16.4 CAR with CD28/CD3 ζ signaling domains exhibited approximately one log₁₀ higher surface CAR expression than T cells transduced with the 7.16.4 4-1BB/CD3 ζ CAR (figure 2B) and produced more IFN- γ and IL-2, proliferated robustly, and exhibited stronger cytotoxicity following co-culture with KP^{mHER2} (figure 2C–E). 7.16.4 HL 28 ζ CAR T (henceforward 7.16.4 CAR T) recognized KP^{mHER2} and not parental KP cells as measured by T-cell cytokine production, proliferation, and tumor cell lysis (figure 2C–G).

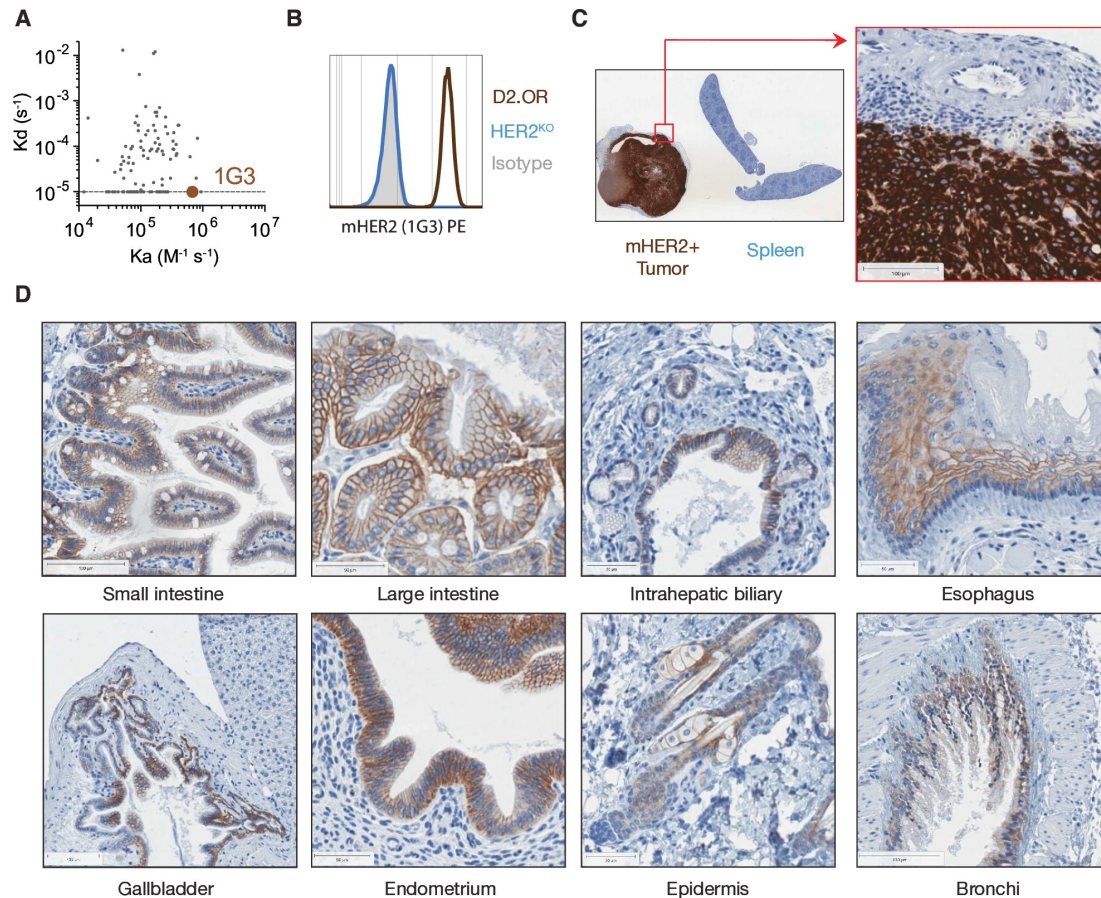


Figure 1 Murine HER2 is expressed in similar normal tissues as human HER2. (A) Plot showing the association (K_a) and dissociation (K_d) constants of binding of individual antibodies to mHER2-hFc. Clone 1G3 is highlighted in brown. Line denotes K_d of $1E^{-5} S^{-1}$, the limit for undetectable dissociation within 600 s. (B) Flow-cytometric analysis of D2.0R cells (brown) and mHER2-knockout D2.0R (blue) stained with 1G3 followed by PE anti-rat antibody. (C) Representative IHC staining with 1G3 for mHER2 on subcutaneously engrafted $Kras^{G12D}/P53^{null}$ (KP) murine lung cancer cells transduced with mHER2 (KP^{mHER2}). Co-embedded spleen was used as HER2-negative control. The inset shows a high-magnification field of the tumor margins. (D) Representative IHC staining with 1G3 on the epithelial tissues of the gastrointestinal tract, liver, uterus, skin, kidney, lung, thymus, and brain of a 6-week-old C57BL/6J female. IHC, immunohistochemistry; HER2, human epidermal growth factor receptor 2; mHER2, murine HER2.

We implanted KP^{mHER2} into mice and 7 days later administered cyclophosphamide (Cy) for lymphodepletion, followed by 1×10^6 70.16.4 CAR T or control T cells transduced with a signaling-deficient CAR (Ctrl T) (figure 2H). 7.16.4 CAR T were safe apart from a transient, mild loss in body weight, also observed in mice receiving Ctrl T (figure 2I). Despite the low dose of 7.16.4 CAR T, tumor growth was significantly inhibited compared with mice that received Ctrl T over the first 21 days (figure 2J). Analysis of tumors at day 23 showed greater CAR T infiltration than Ctrl T (figure 2K). A subsequent experiment of longer duration to confirm the safety of 7.16.4 CAR T resulted in a survival benefit, however tumors progressed after day 60. Progressing tumors had lower levels of mHER2 by IHC compared with tumors in Ctrl T treated mice, consistent with immune editing of high-mHER2-expressing tumor cells by 7.16.4 CAR T (figure 2L and M).

We next evaluated 7.16.4 CAR T in the B16F10 model, which is known to rapidly induce T-cell exhaustion.³⁵

Because parental B16F10 expresses very low endogenous levels of mHER2, we generated a B16F10 line ($B16^{mHER2}$) that expressed higher levels of mHER2 by transduction (online supplemental figure 3A). Mice were engrafted with $B16^{mHER2}$ and treated 10 days later with Cy and 1×10^6 70.16.4 CAR T (online supplemental figure 3A). $B16^{mHER2}$ growth was only transiently delayed and survival was not improved (online supplemental figure 3B). In a second experiment, we engrafted $B16^{mHER2}$ and B16 parental tumors to examine tumor infiltration and escape mechanisms. 7.16.4 CAR T infiltrated $B16^{mHER2}$ but not parental B16 (online supplemental figure 3C), however mHER2 expression was not decreased on persisting $B16^{mHER2}$ (online supplemental figure 3D). Instead, as reported previously,³⁵ tumor-infiltrating CAR T upregulated inhibitory receptors and exhibited decreased IL-2 production (online supplemental figure 3E and F). These data demonstrate that mHER2-specific CAR T can target tumors expressing high levels of HER2 without toxicity, and identify tumor model dependent escape mechanisms.

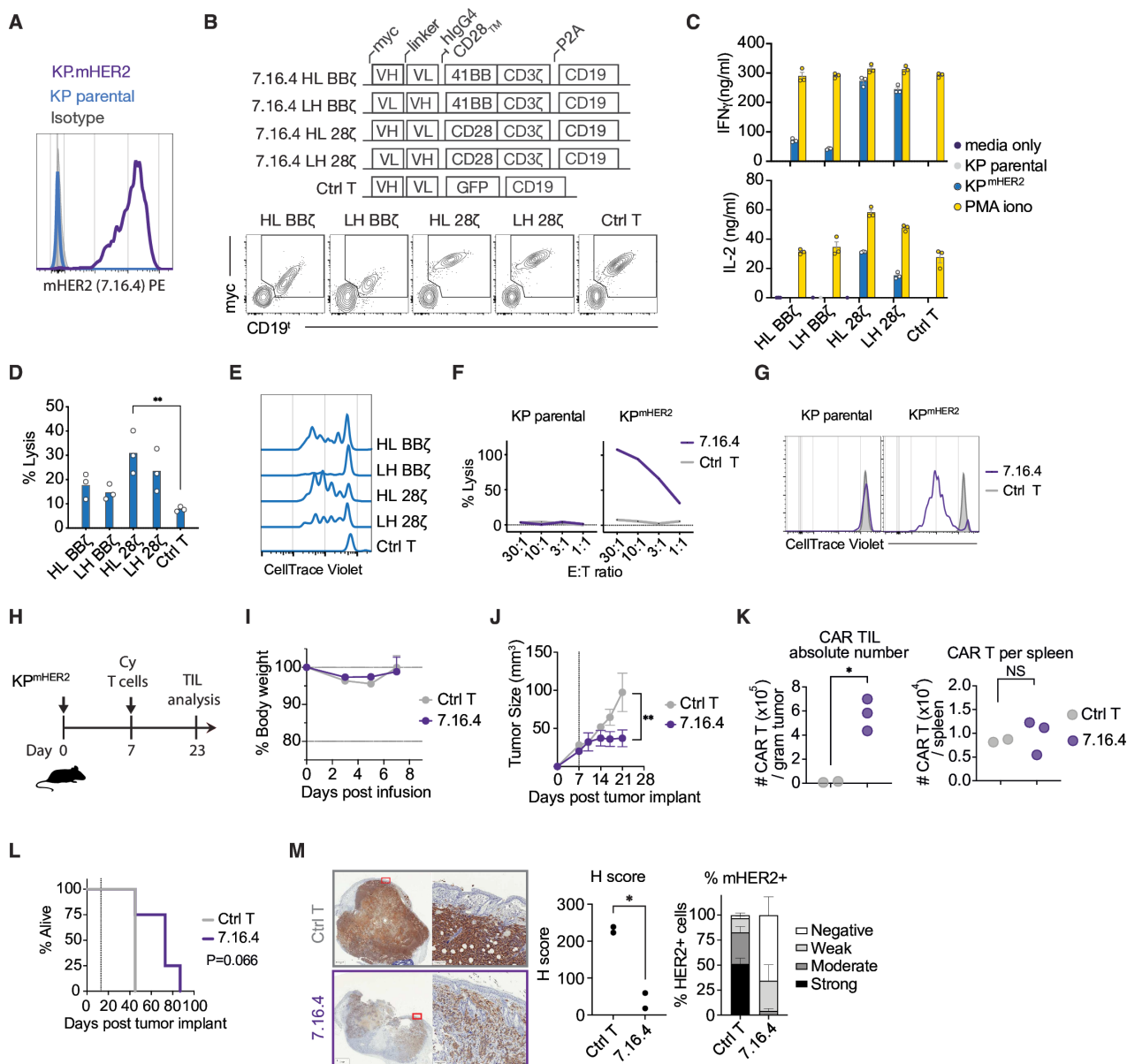


Figure 2 Low-affinity mHER2 CAR T cells eliminate HER2-high tumor cells and spare normal HER2+ tissues. (A) Flow cytometric analysis of parental KP cells and KP cells transduced with mHER2 (KP^{mHER2}) stained with PE-conjugated anti-rat HER2 7.16.4 or mouse IgG2a, κ isotype (gray). (B) Top: schematic of constructs encoding CARs and signaling-deficient control variant. Bottom: Expression of CAR (myc) and transduction marker (CD19⁺) evaluated by 96 hours after transduction. (C) IFN- γ (top) and IL-2 (bottom) levels measured by ELISA in supernatants collected at 24 hours from co-cultures of CAR T cells (E:T=2:1) with the indicated tumor cell lines. Absence of symbols indicates values below detection limit. Maximal stimulation with PMA and ionomycin is shown as a positive control. (D) Percentage lysis of ⁵¹Cr-labeled tumor cells after 4 hours of co-culture with CAR T cells and KP^{mHER2} cells at 10:1 ratio. (E) Proliferation of CAR T cells after stimulation with KP^{mHER2} cells (E:T=2:1, 48 hours). (F) Percentage lysis of ⁵¹Cr-labeled tumor cells after 24 hours of co-culture with 7.16.4 28 ζ CAR or control T cells and target cells at indicated E:T ratios. (G) Proliferation of 7.16.4 HL.28 ζ CAR T cells or control T cells after stimulation with target cells (E:T=2:1, 48 hours). (H) Adoptive transfer protocol: mice were implanted subcutaneously with 2×10^5 KP^{mHER2} tumor cells, administered 200 mg/kg cyclophosphamide (Cy) 7 days post implantation, and 6 hours later given 1×10^6 CD45.1+ CAR T cells or control T cells. (I) Body weight changes of tumor-bearing mice after treatment. (J) KP^{mHER2} tumor volumes after treatment with 7.16.4 HL.28 ζ CAR or control T cells. (K) Absolute numbers of CD19⁺ CAR T cells, gated on CD8+CD45.1+ cells in tumors and spleens from KP^{mHER2} tumor-bearing mice analyzed on day 23. (L) Survival of tumor-bearing mice treated with 7.16.4 HL.28 ζ CAR or control T cells. Tumors were harvested for (M) when they ulcerated or reached size limit. (M) Representative immunohistochemistry staining for mHER2 expression in KP^{mHER2} tumors (left) and quantification of expression (right). Symbols represent technical replicates (C, D) or individual mice (K, M), and symbols or bars with error bars represent means \pm SEM (I–M) with $n=2-3$ mice per group and (I–K) $n=3-4$ mice per group (L). *, $p < 0.05$, t-test (K, M) or analysis of variance (Šidák post hoc (J) or Tukey post hoc (D)). Log-rank test (L). CAR, chimeric antigen receptor; E:T, effector to target; IFN, interferon; IL, interleukin; HER2, human epidermal growth factor receptor 2; mHER2, murine HER2; PMA, phorbol myristate acetate; TIL, tumor-infiltrating lymphocyte.

High-affinity mHER2-specific CAR T causes toxicity without improving antitumor efficacy

The 7.16.4 IgG has low affinity for mHER2,³⁴ which may contribute to escape of HER2-low tumor cells and to T-cell exhaustion. We screened our antibody library to identify mHER2-specific scFvs with higher affinity than 7.16.4. Because 7.16.4 competes with Herceptin for binding to membrane-proximal domain IV on hHER2 (figure 3A),³⁶ we limited analysis to scFvs that recognize domain IV of mHER2 (aa490-631) to exclude potential effects on CAR T activation of targeting membrane-distal epitopes.³⁷ We identified 34 antibodies that bound domain IV with a wide range (10 pM – 10 μM) of affinities (figure 3B, online supplemental table 2). All but one of these IgGs exhibited superior binding to mHER2+D2.OR murine breast cancer cells compared with 7.16.4 (figure 3C,D).

Based on affinity measurements and off-rates, we selected clones 1G3 (K_D 682pM), previously used for IHC (figure 1), and 1C9 (K_D 18pM) to construct CD28/CD3ζCARs (figure 3E). Compared with the 7.16.4 CAR, the 1G3 CAR had lower cell-surface expression on T cells in both variable fragment heavy chain and light chain (HL) and variable fragment light chain and heavy chain (LH) formats compared with the 7.16.4 CAR, while the 1C9 CAR was expressed at similar levels in the LH format (figure 3E). Consistent with the superior EC_{50} for binding to D2.OR, we observed an approximately three-log reduction in the amount of plate-bound HER2 required to elicit cytokine production by 1G3 HL, 1G3 LH, and 1C9 LH CAR T compared with 7.16.4 CAR T (figure 3F). The 1C9 HL CAR, which had low T cells expression, recognized plate bound mHER2 poorly and was excluded from further analysis. T cells expressing 1G3 HL and 1C9 LH CARs produced IFN-γ and proliferated when co-cultured with tumor cells expressing high, intermediate, or low levels of mHER2 (figure 3G–I). By contrast, 7.16.4 and 1G3 LH CAR T responded only to tumor cells expressing intermediate and high levels of antigen, confirming the greater sensitivity of the 1G3 HL and 1C9 LH CARs for HER2-low tumor (figure 3G–I). 1G3 HL and 1C9 LH CAR T also completely lysed tumor cells expressing intermediate HER2 levels, whereas 7.16.4 CAR T only lysed tumor cells with high HER2 levels (figure 3J). 1C9 LH CAR T did not kill mHER2^{KO} D2.OR, demonstrating specificity for mHER2 (figure 3K).

To determine the safety and efficacy of high-affinity HER2 CAR T, we treated mice bearing parental B16F10 tumors expressing low endogenous levels of mHER2 and mice bearing B16F10^{mHER2} tumors with 7.16.4, 1G3 HL, and 1C9 LH CAR T (1×10^6) after Cy lymphodepletion (figure 4A). 7.16.4 CAR or Ctrl T resulted in minimal weight loss and no toxicity as before, whereas 1G3 HL CAR T elicited moderate weight loss and 1C9 LH CAR T elicited severe weight loss, requiring euthanasia of most mice by day eight post infusion (figure 4B). The number of 7.16.4, 1G3 HL, and 1C9 LH CAR T in the spleens of treated mice was similar, however a higher frequency of splenic 1G3 HL and 1C9 LH CAR T expressed

programmed cell death protein 1 (PD-1), T cell immunoglobulin and mucin domain-containing protein 3 (Tim-3), and CD39 compared with 7.16.4 CAR T (figure 4C, online supplemental figure 4A and B). High-affinity 1G3 HL and 1C9 LH CAR T infiltrated both the mHER2-low parental and mHER2-high tumors while the low-affinity 7.16.4 CAR T infiltrated mHER2-high tumors better than mHER2-low tumors (figure 4D). PD-1, Tim-3, and CD39 were upregulated on tumor-infiltrating CAR T in all cohorts (figure 4D, online supplemental figure 4C). 1C9 LH CAR T resulted in early lethal toxicity precluding analysis of antitumor activity. However, the high affinity 1G3 HL CAR T provided no discernible survival benefit over 7.16.4 CAR T and Ctrl T, with all mice succumbing to tumor by day 42 (figure 4E). These data indicate that despite superior recognition of HER2 in vitro, high-affinity HER2-targeted CAR T elicited overt, moderate-to-severe toxicity, acquired an exhaustion signature, and failed to improve antitumor activity against HER2+B16F10 tumors in vivo.

High-affinity CAR T cells infiltrated both low and high HER2 tumors and exhibited more robust accumulation in the mHER2-high tumors, suggesting that HER2 expression on the tumor might drive CAR T expansion and contribute to toxicity. We therefore tested whether 1C9 LH CAR T would elicit toxicity in non-tumor-bearing mice and whether toxicity was related to T-cell dose and/or lymphodepleting chemotherapy. Normal mice infused with 1×10^7 1C9LH CAR T after lymphodepleting chemotherapy exhibited high CAR T levels in blood and severe weight loss, whereas mice that received the same CAR T dose without lymphodepleting chemotherapy had a low frequency of CAR T in blood and no toxicity (figure 5A). The severity of toxicity in mice receiving lymphodepletion was also related to the dose of 1C9 LH CAR T and correlated with the peak CAR T frequency in blood (figure 5A). We tested various doses of Cy or radiation for lymphodepletion prior to an intermediate dose (3×10^6) of 1C9 LH CAR T and found that more intense lymphodepletion resulted in higher peak blood CAR T levels and greater toxicity (figure 5B,C). Mice that developed severe toxicity after 1C9 LH CAR T had marked increases in serum tumor necrosis factor alpha (TNF-α) and IFN-γ and elevated levels of chemokines associated with effector T-cell trafficking compared with control mice or mice treated with 7.16.4 CAR T (figure 5D). Liver dysfunction and malnutrition were evident in mice treated with 1C9 LH CAR T and correlated with severity of weight loss 1-week post infusion (figure 5E). Further, analysis of the small intestine identified overt histologic damage in mice that developed severe toxicity after lymphodepletion and 3×10^6 1C9LH CAR T including elongation of the crypts of Lieberkuhn and villus fusion and blunting (figure 5F). We examined three normal HER2⁺ tissues and found significantly higher infiltration by CD3+lymphocytes in the lungs and uterus and a trend towards higher levels in the small intestine of mice treated with 3×10^6 1C9LH CAR T after high dose Cy lymphodepletion (figure 5G).

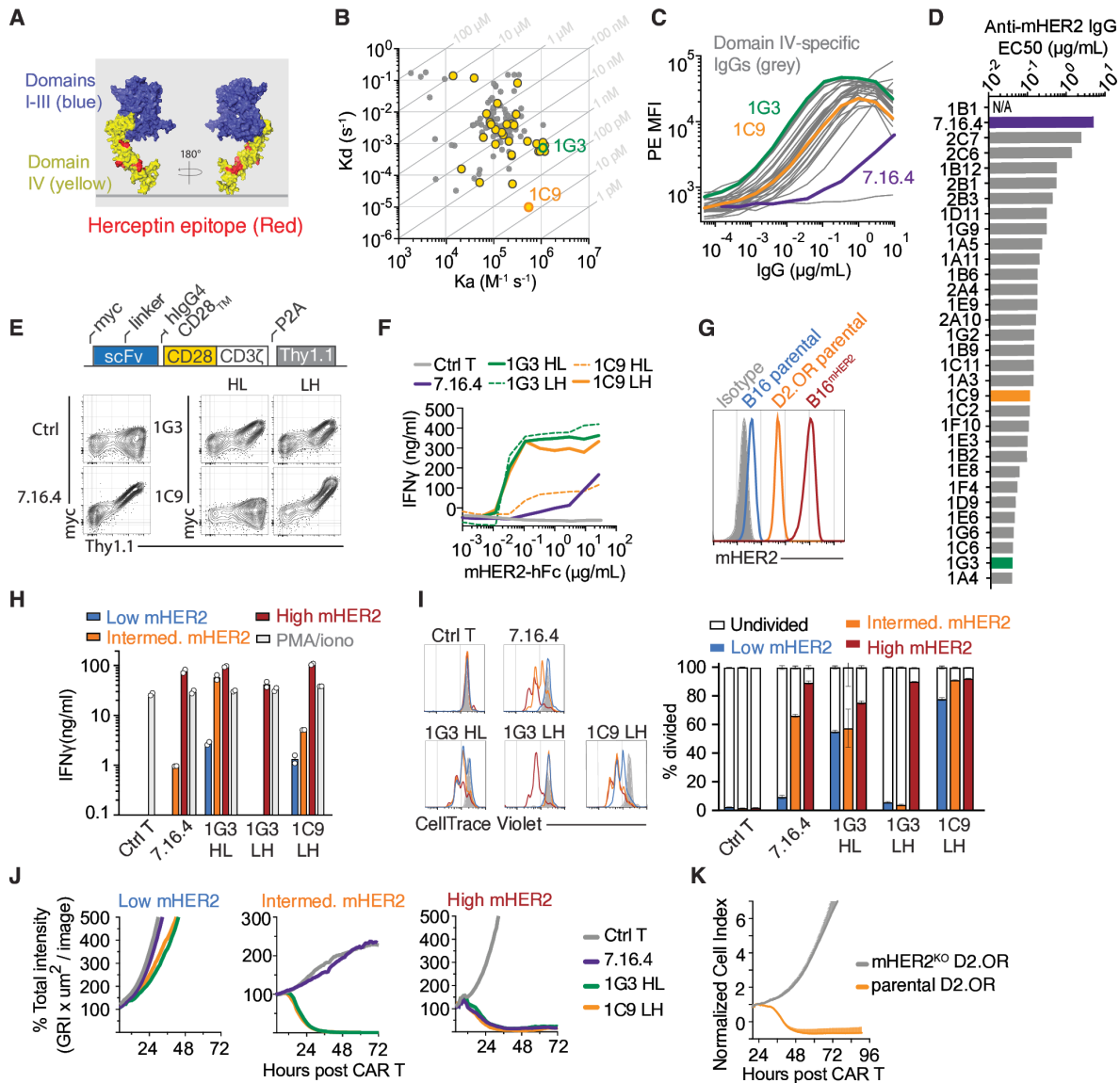


Figure 3 Enhancing the CAR affinity lowers the antigen threshold for T-cell activation in vitro. (A) Alpha-fold model of human HER extracellular domain (AF-P70424-F1) with domain IV in yellow and the 3D epitope of trastuzumab, as previously reported,⁴⁷ highlighted in red. (B) Isoaffinity plot showing association (K_a) and dissociation (K_d) constants of binding of various antibodies to immobilized monomeric mHER2.His, with diagonal lines representing the equilibrium constants (K_D). Yellow symbols indicate clones that bind both the full extracellular domain and domain-IV of mHER2 (see online supplemental table 2 for values). Clones 1G3 and 1C9 are highlighted in green and orange, respectively. (C) Sigmoidal binding of mHER2-domain-IV-specific antibodies to parental D2.0R cells determined by flow cytometry after staining with the respective IgG followed by PE anti-rat antibody. (D) Calculated EC_{50} values of anti-mHER2 IgGs for binding to D2.0R. “N/A” denotes inability to calculate EC_{50} due to poor binding. (E) Top: schematic of constructs encoding mHER2 CARs. Bottom: expression of 1G3 and 1C9 CARs in the HL and LH formats measured by staining for the myc tag, compared with 7.16.4 HL CAR and transduction-marker-only control T cells. (F) IFN- γ levels measured by ELISA in the supernatants of the indicated CAR T cells stimulated for 24 hours with solid phase-coated mHER2. (G) Flow cytometric analysis of mHER2 expression on parental B16, parental D2.0R, and mHER2-high B16 tumor cells after staining with 1G3 or isotype control (gray). (H) IFN- γ levels measured by ELISA in supernatants of co-cultures of the indicated CAR T cells and parental B16, parental D2.0R, and B16^{mHER2} tumor cells (E:T=2:1, 24 hours) expressing low, intermediate, or high levels of mHER2, respectively. Maximal stimulation with PMA and ionomycin used as a positive control. (I) Proliferation of indicated CAR T cells after stimulation with parental B16, parental D2.0R, and B16^{mHER2} target cells (E:T=2:1, 48 hours). Left: CellTrace Violet dilution at 48 hours. Right: Bar graph showing % of CAR T cells undergoing at least one division. (J) Fluorescence-based cytotoxicity assay measuring the cytotoxicity of indicated CAR T cells against target cells expressing low, intermediate, or high levels of mHER2 (E:T=10:1). (K) Impedance-based cytotoxicity assay measuring cytolytic activity of 1C9.LH CAR T cells against wild-type or mHER2^{KO} D2.0R cells at E:T ratio of 10:1. Symbols represent technical replicates (H) and bars with error bars represent means \pm SEM (I) with n=3 (H–K). CAR, chimeric antigen receptor; E:T, effector to target; IFN, interferon; HER2, human epidermal growth factor receptor 2; HL, variable fragment heavy chain and light chain; LH, variable fragment light chain and heavy chain; MFI, mean fluorescence intensity; mHER2, murine HER2; PMA, phorbol myristate acetate.

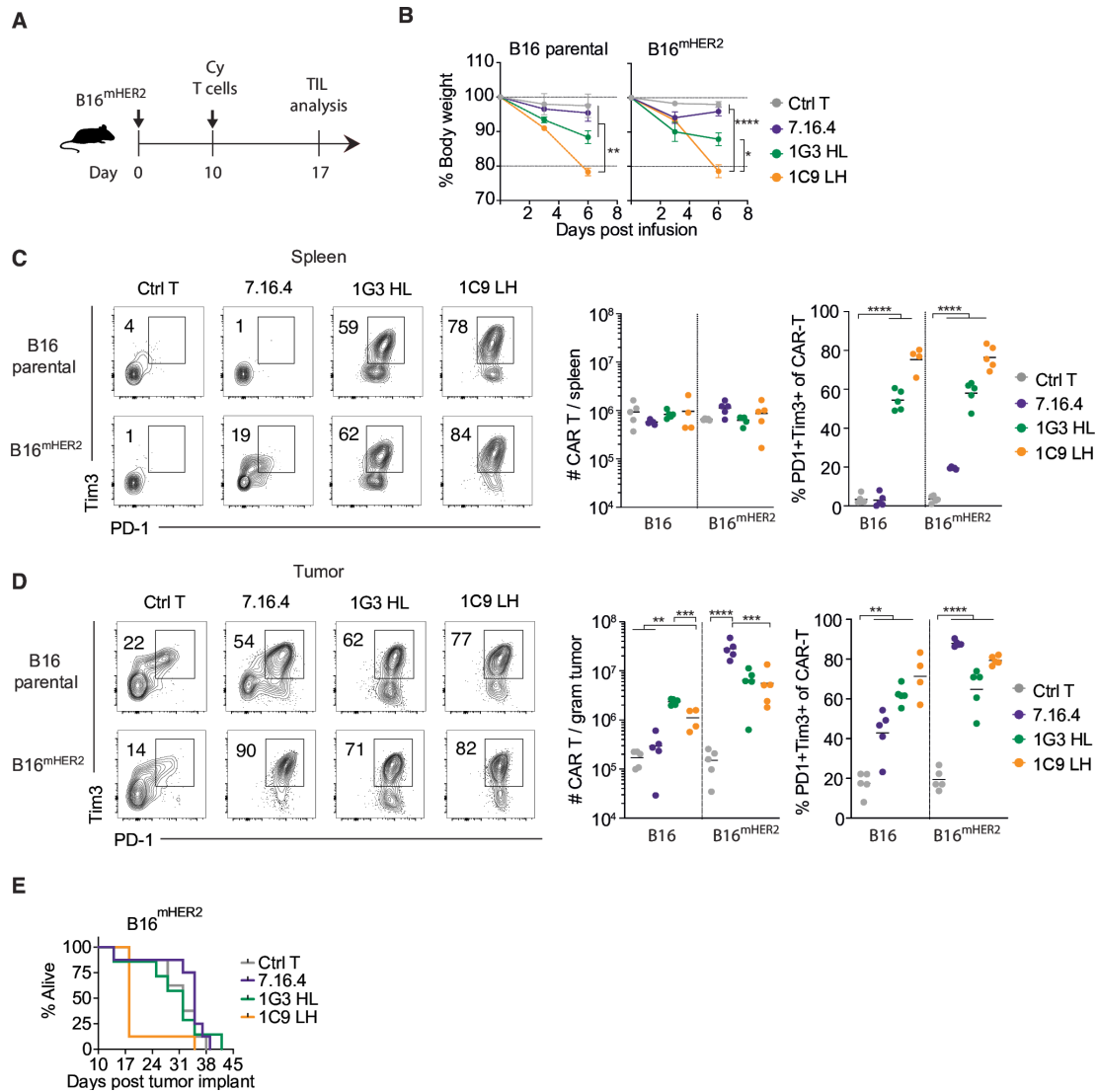


Figure 4 High-affinity mHER2.CAR T cells do not improve antitumor function in vivo and elicit on-target off-tumor toxicity. (A) Schematic of adoptive transfer protocol. Cohorts of mice were implanted subcutaneously with 4×10^5 B16 parental or B16^{mHER2} tumor cells, administered 200 mg/kg cyclophosphamide (Cy) 10 days post tumor implantation and 6 hour later given 1×10^6 CD45.1+ CAR T cells or control T cells. (B) Average body weight changes relative to baseline in parental B16 or B16^{mHER2} tumor-bearing mice. (C–D) Mice were sacrificed on day eight post infusion and flow cytometry was used to determine the absolute number of Thy1.1+ CAR T cells and their dual expression of PD-1 and Tim-3 in the spleens (C) and tumors (D) of tumor-bearing mice treated with the indicated CAR T cells. (E) Survival curves of tumor-bearing mice treated with the indicated CAR T cells. Symbols with error bars represent means \pm SEM (B) and symbols represent individual mice (C,D) with $n=4-5$ mice per group (B–D) 7–8 (E). * <0.05 , ** <0.01 , *** <0.001 , **** <0.0001 by analysis of variance (Dunnett post hoc) (B–D). CAR, chimeric antigen receptor; E:T, effector to target; HL, variable fragment heavy chain and light chain; LH, variable fragment light chain and heavy chain; mHER2, murine human epidermal growth factor receptor 2; PD-1, programmed cell death receptor 1; TIL, tumor-infiltrating lymphocyte; Tim-3, T cell immunoglobulin and mucin domain-containing protein 3.

A subsequent study using flow cytometry to detect CAR T confirmed that mice treated with higher Cy exhibited significant 1C9 LH CAR T-cell infiltration in the lung and intestine, while mice treated with a low dose of Cy exhibited CAR T infiltration in these organs similar to that observed with Ctrl T (figure 5H). Thus, OTOT toxicity induced by high-affinity HER2-specific CAR T is independent of the presence of HER2⁺ tumor and correlated with CAR T dose, lymphodepletion intensity, and systemic proliferation of CAR T.

Selection of moderate affinity mHER2 CARs with low in vivo toxicity does not improve antitumor efficacy

Antitumor efficacy superior to 7.16.4 CAR T might be achieved with alternative CARs without eliciting the toxicity observed with the high-affinity 1G3 HL and 1C9 LH CARs. We therefore screened CD28 ζ CARs constructed from the 38 domain IV-directed scFvs for toxicity in normal non-tumor-bearing mice following lymphodepletion (figure 6A). To facilitate lymphodepletion of a large number of mice, we used 500 cGy irradiation, which

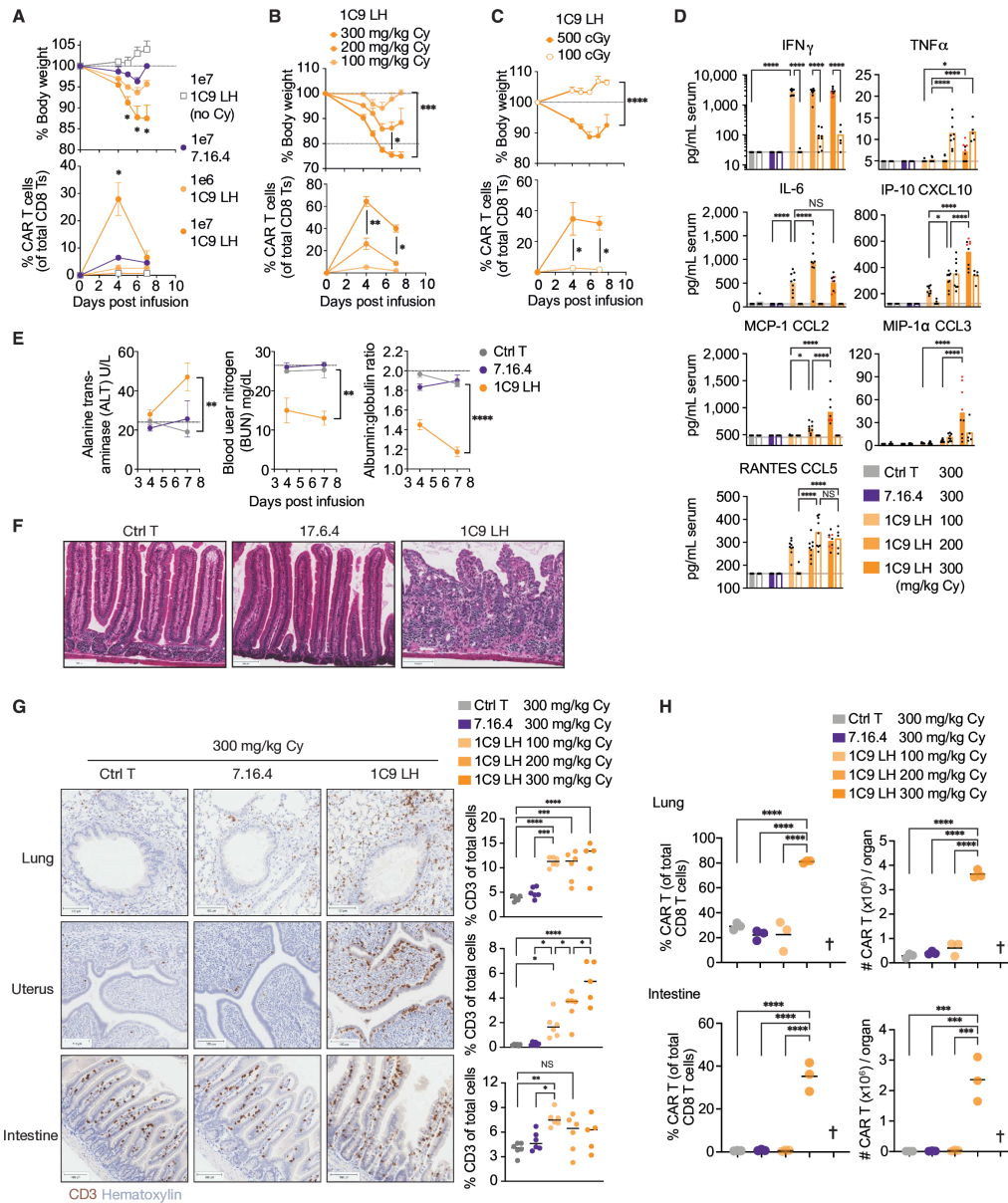


Figure 5 Factors that affect off-tumor on-target toxicity of mHER2.CAR T cells. (A) Top: average body weight changes in mice treated with 200 mg/kg Cy (unless otherwise stated) prior to infusion with the indicated number of CAR T cells. Bottom: frequency of CAR T cells relative to total CD8⁺ T cells in blood in each group of mice. Dashed lines represent the starting weight (100%) and the endpoint requiring euthanasia (80%). (B–C) Top: average body weight changes in mice treated with various doses of Cy (B) or total body radiation (C) prior to infusion of 3 × 10⁶ CAR T cells. Bottom: frequency of CAR T cells relative to total CD8⁺ T cells in blood. (D) Cytokine levels on day 4 (solid color) and 8 (outlined color) by Mouse Luminex Discovery Assay in serum of mice treated with indicated lymphodepletion regimen prior to infusion with 3 × 10⁶ CAR T cells. Red symbols indicate 1C9 LH cohort mice that died post day 4. (E) Serum chemistry analysis on day 7 in mice treated with 200 mg/kg Cy and infused with 1 × 10⁷ CAR T cells. (F) Representative H&E stains of small intestine on day 7 from mice treated with 200 mg/kg Cy and 3 × 10⁶ control, 7.16.4, or 1C9 LH CAR T cells. (G) Left: representative IHC staining of CD3+lymphocytes in lung, uterus, and intestinal tissues. Mice were treated with various doses of Cy and infused with 3 × 10⁶ CAR T cells and tissues were harvested on day 8 post infusion. Right: percentage of CD3+cells relative to the total number of cells on the stained slide. (H) Lungs and small intestines from mice treated as in (D) and analyzed by flow cytometry on day 8 for the percentage and absolute numbers of Thy1.1+ CART cells, gated on CD8+CD45.1+ cells. †Indicates that mice died prior to tissue harvest and were not analyzed. Symbols represent individual mice (D, G, H) and symbols with error bars represent means ± SEM (A–C, E) with n=3 mice per group (A–C, E) n=5–9 mice per group (D) or n=5–6 mice per group (G). * < 0.05, ** < 0.01, *** < 0.001, **** < 0.0001 by analysis of variance with Dunnett post hoc (A–B) Sidak post hoc (C) top, (E, H) Bonferroni post hoc (C) bottom, or Tukey post hoc (D, G). Line represents the Luminex limit of detection (D) or levels measured in untreated mice (E) mean of n=3. CAR, chimeric antigen receptor; CCL, C-C motif chemokine ligand; CXCL, C-X-C motif chemokine ligand; Cy, cyclophosphamide; HL, variable fragment heavy chain and light chain; IFN, interferon; IL, interleukin; IP, intraperitoneal; LH, variable fragment light chain and heavy chain; mHER2, murine human epidermal growth factor receptor 2; MCP, monocyte chemoattractant protein; MIP, macrophage inflammatory protein; TNF, tumor necrosis factor.

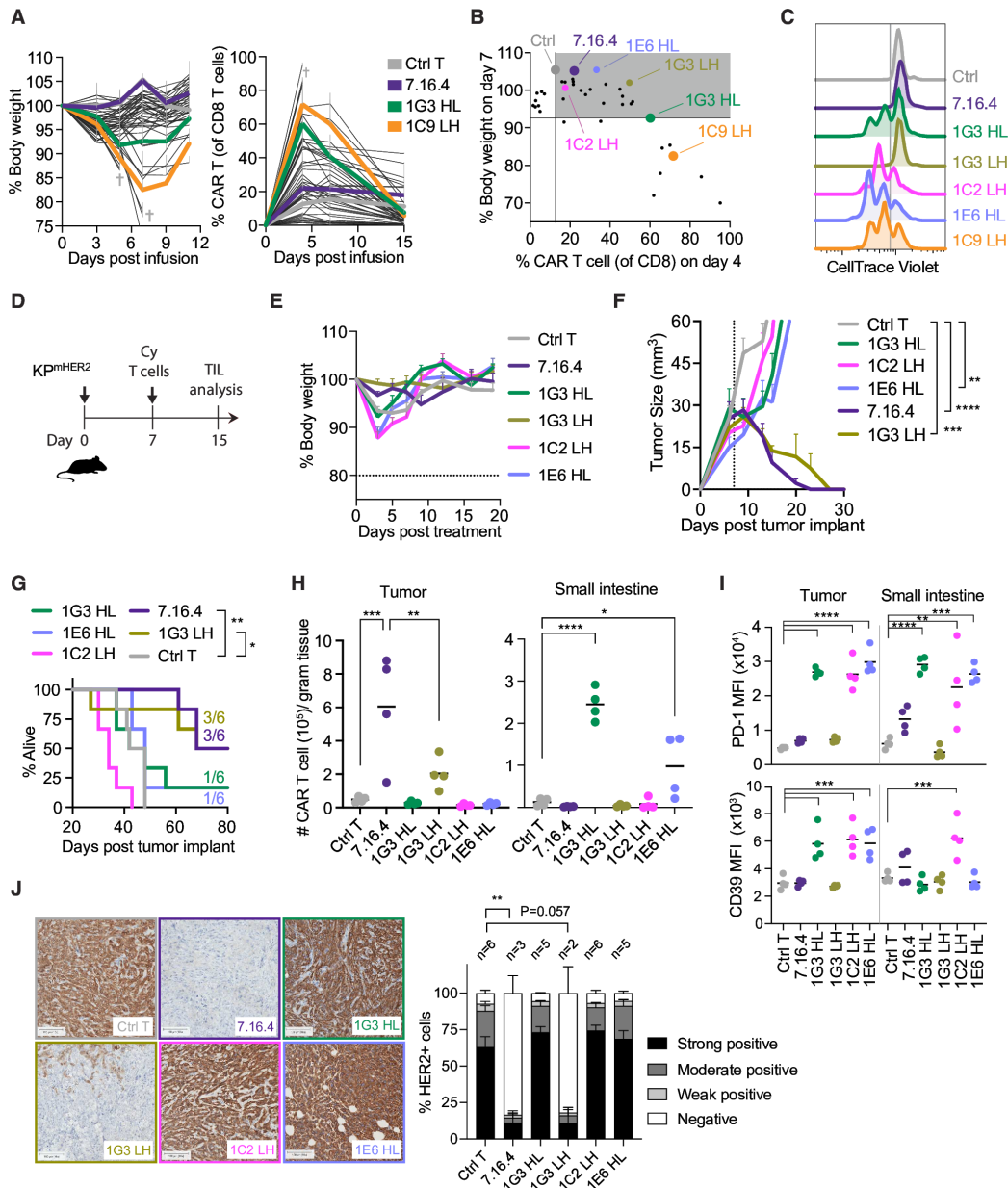


Figure 6 Selection of higher-affinity mHER2 CARs with intrinsically low in vivo toxicity does not improve antitumor efficacy. (A) Left: average body weight changes in mice treated with 500 cGy prior to infusion with 3×10^6 mHER2 domain-IV-specific CAR T cells. Right: frequency of CAR T cells relative to total CD8⁺ T cells in blood. Truncated lines and † indicate lethality. (B) Plot derived from (A) correlating the average body weight on day 7 with the frequency of CAR T cells in blood on day 4. $R^2=0.5101$. Shaded area indicates CAR T cells with blood expansion that is superior to Ctrl T cells and lower toxicity than 1G3 HL. (C) Proliferation of CAR T cells after stimulation low-mHER2 target cells (E:T=2:1, 48 hours). See online supplemental table 3 for details. (D) Schematic of adoptive transfer protocol. Cohorts of 6 mice per group were implanted subcutaneously with 2×10^5 KP^{mHER2} tumor cells, administered 200 mg/kg cyclophosphamide (Cy) 7 days post tumor implantation and 6 hours later given 3×10^6 CD45.1+ CART cells or control T cells. (E) Average body weight changes relative to baseline. (F) KP^{mHER2} tumor volumes post treatment with indicated CAR or control T cells and statistics shown for day 15 post tumor implant. (G) Survival of KP^{mHER2} tumor-bearing mice treated with CAR or control T cells. Tumors were harvested for (J) when they ulcerated or reached size limit. Fractions indicate the number of tumor-free mice at end of study (day 85). (H–I) Mice were sacrificed on day 8 post infusion and flow cytometry was used to determine the absolute numbers of Thy1.1+ CAR T cells, gated on CD8+CD45.1+ cells (H) and expression levels of PD-1 and CD39 (I). (J) Representative IHC staining (left) and quantification (right) for mHER2 expression in KP^{mHER2} tumors harvested on the euthanasia end points indicated in (G). The number of tumors processed for IHC is indicated. Lines with error bars represent means \pm SEM (A,E,F) and symbols represent individual mice (H,I) and with n=3 mice per group (A,B) n=6 mice per group (E–G) or n=4 mice per group (H,I). * <0.05 , ** <0.01 , *** <0.001 , **** <0.0001 by ANOVA with Dunnett (F,I) or Tukey (H) post hoc, log-rank test (G) or ANOVA with Fisher’s LSD test (J). ANOVA, analysis of variance; CAR, chimeric antigen receptor; E:T, effector to target; HER2, human epidermal growth factor receptor 2; HL, variable fragment heavy chain and light chain; IHC, immunohistochemistry; LH, variable fragment light chain and heavy chain; MFI, mean fluorescence intensity; mHER2, murine HER2; PD-1, programmed cell death receptor 1; TIL, tumor-infiltrating lymphocytes.

previously elicited weight loss in 1C9 LH CAR T treated mice comparable to pretreatment with 200mg/kg Cy (figure 4B,C). We observed a range of weight loss and CAR T expansion in blood, and a correlation emerged between CAR T expansion 4days post infusion and severity of weight loss (figure 6A,B). 1C2 LH (1C2 - K_D 57nM) and 1E6 HL (1E6 - K_D 604 pM) CAR T expanded better in vivo than Ctrl T but caused less toxicity than 1G3 HL CAR T (figure 6B). When co-cultured in vitro with tumor cells expressing low mHER2, 1C2 LH and 1E6 HL CAR T exhibited robust proliferation, cytokine production, and cytotoxicity that was comparable to 1G3 HL and 1C9 LH CAR T and superior to T cells expressing the 7.16.4 CAR or a 1G3 CAR formatted in an LH configuration (figure 6C, online supplemental table 3).

We then analyzed 1C2 LH and 1E6 HL CAR T for anti-tumor activity in mice bearing KP^{mHER2} and also included CAR T expressing the 1G3 LH variant, which required a higher antigen threshold for activation (figure 3H,I). Mice were engrafted with KP^{mHER2} and 7 days later administered Cy followed by 3×10^6 CAR or Ctrl T (figure 6D). The infusion of 1G3 HL, 1E6 HL, or 1C2 LH CAR T into tumor-bearing mice elicited mild transient weight loss that was greater than observed with irradiation in non-tumor bearing mice, and greater than observed with 1G3 LH and 7.16.4 CAR T (figure 6E). Despite the absence of toxicity and superior recognition of mHER2-low tumor cells in vitro, 1E6 HL or 1C2 LH CAR T did not control the tumor nor provide a survival advantage compared with Ctrl T (figure 6F,G). However, all mice treated with 7.16.4 or with 1G3 LH CAR T, which were less able to recognize tumor cells expressing low levels of mHER2 in vitro than 1E6 HL, 1C2 LH, and 1G3 HL CAR T, had significant reduction in tumor size and 50% of mice exhibited complete tumor elimination resulting in enhanced survival (figure 6F,G).

A concurrent cohort of tumor-bearing mice was treated identically for analysis of tumor and tissue sites. 1G3 LH and 7.16.4 CAR T infiltrated the tumor but not the small intestine, whereas 1G3 HL and 1E6 HL CAR T that caused the greatest weight loss accumulated in the small intestine but did not infiltrate the tumor (figure 6H). In contrast to the infiltration of $B16^{mHER2}$ tumors observed previously (figure 4D), 1G3 HL CAR T did not infiltrate KP^{mHER2} tumors any more than Ctrl T, suggesting that tumor trafficking and/or retention at the tumor site can be tumor model specific. 1C2 LH CAR T did not accumulate in the tumor or small intestine and mortality was due to tumor ulceration (figure 6F–H). Phenotypic analysis of 1G3 HL, 1C2 LH, and 1E6 HL CAR T present in the tumor and intestine showed significant increases in PD-1, CD39, and Tim-3 (figure 6I, online supplemental figure 5). Moreover, IHC of tumors in mice that progressed revealed drastically lower levels of mHER2 expression in the 7.16.4 and 1G3 LH groups compared with tumors harvested at euthanasia from mice treated with the higher affinity 1G3 HL, 1C6 LH, 1E6 HL CAR T, or with Ctrl T (figure 6J).

This demonstrates that HER2 CAR T designed from scFvs with low affinity or from higher affinity scFvs in less active formats can safely mediate potent antitumor activity against tumor cells that express high levels of HER2. These studies also demonstrate that the deliberate selection of moderate-affinity CARs with superior responses in vitro to low-antigen tumor cells did not improve the antitumor efficacy of CAR T therapy, due to inefficient trafficking to the tumor and diversion to normal tissues that express HER2.

DISCUSSION

A challenge for CAR T therapy of epithelial cancers is the paucity of cell-surface molecules restricted only to the tumor. Factors governing the potential for OTOT toxicity for individual target antigens are difficult to predict or to define in small clinical trials that differ in CAR design, manufacturing methods, preconditioning, CAR T-cell dose, and tumor histology, burden, and location. Our studies in a physiologically relevant murine model illustrate the difficulty of achieving adequate safety and anti-tumor efficacy with high-affinity HER2 CAR T. We find the development and severity of OTOT toxicity is influenced by HER2 CAR affinity, cell dose, and intensity of lymphodepletion. Even CARs that recognize tumor cells in vitro and exhibit an adequate safety profile in vivo lack the desired antitumor activity, due to poor trafficking to tumor sites, diversion to normal tissues and/or the development of T-cell exhaustion. Despite these barriers, a therapeutic window for targeting tumors that express high levels of HER2 can be achieved using low-affinity CAR T cells.

The lack of immunocompetent models has hindered preclinical analysis of HER2-directed CAR T therapies. Previously, murine models have employed strategies to express hHER2 but fail to recapitulate physiologic expression levels and tissue locations of HER2 in humans. Meanwhile, the lack of preclinical reagents for assessing the tissue expression of mHER2 and designing mHER2-directed CARs hindered the use of fully immunocompetent mice for OTOT toxicity. We developed an HER2-specific antibody for characterization of mHER2 expression and demonstrated that expression patterns are highly similar in humans. Constructing CARs from antibodies with a range of affinities for mHER2 allowed a reductionist assessment of the role of CAR affinity, conditioning regimens, and T-cell dose in OTOT toxicity. Increasing mHER2 CAR affinity lowered the antigen threshold for CAR T recognition. In vitro, CAR T constructed from mHER2-specific IgGs with subnanomolar affinity recognized HER2-low tumor cells better than low affinity 7.16.4 CAR T, without losing specificity. These findings are consistent with previous studies that described the lower antigen thresholds of high-affinity hHER2-targeting or GD2-targeting CARs in vitro.^{27 38} However, when high-affinity HER2 CAR T were administered in vivo, many variants elicited lethal OTOT toxicity,

consistent with the fatal toxicity observed in a patient treated with CAR T constructed from the high-affinity trastuzumab.²³ Our murine model partially recapitulates the pathology revealed in the patient postmortem, including elevated serum TNF- α and IFN- γ levels and severe intestinal damage.²³ Although lymphodepletion improves the antitumor efficacy of adoptive T-cell transfer in preclinical models and in patients,^{39–41} our studies identified a link between lymphodepletion intensity and toxicity when high-affinity HER2 CAR T are used.

While several of our high-affinity CARs elicited severe toxicity, others did not elicit toxicity in vivo despite recognizing mHER2-low tumor cells in vitro, illustrating the challenge of inferring that superior in vitro tumor recognition is predictive of potent CAR T activity in vivo. While 1G3 HL and 1G3 LH exhibited similar activation to plate-bound antigen, 1G3 LH CAR T were less effective in recognizing tumor cells expressing low HER2 levels, underscoring the role of scFv orientation and optimal steric interactions with cell membrane-bound antigen. The functionally restrained 1G3 LH yielded a CAR similar to 7.16.4 for in vitro tumor recognition and efficiently controlled tumor growth in vivo. Finding the CAR “sweet spot” affinity threshold a priori may require empirical testing to identify optimal CAR candidates.

While the therapeutic window of any CAR T may ultimately be patient specific, our studies show that general principles to guide the development of safe CAR T may be elucidated from preclinical models. We found that low-affinity mHER2 CAR T regressed mHER2+ tumors without eliciting discernible toxicity, identifying a potential safe approach for treating HER2-high tumors. The finding that low-affinity mHER2 CAR T cells selectively eliminate HER2-high tumor cells is consistent with a previous report that T cells expressing an affinity-tuned trastuzumab-derived CAR mounted a robust antitumor response against hHER2-high tumor xenografts without affecting the growth of secondary, hHER2-low tumors used as surrogates for normal tissue expression.²⁷ It is notable that even when 7.16.4 and 1G3 LH CAR T cells inhibited tumor growth, tumor resistance mechanisms including antigen-low escape in KP tumors and T-cell exhaustion in B16 tumors enabled subsequent tumor outgrowth. These resistance mechanisms may limit the long-term efficacy of HER2 CAR T in the clinic, as human cancers exhibit significant intratumoral heterogeneity in HER2 expression⁴² and induce T-cell exhaustion.⁴³ Nonetheless, our findings highlight a path forward for targeting solid tumors with high levels of HER2, employing low-affinity CAR T cells that offer both safety and efficacy, and provides the framework for future studies to evaluate targeting heterogeneous antigen expressing tumors. Once safety is established, combinatorial or logic-gated strategies to overcome T-cell dysfunction and antigen escape, respectively, can be evaluated to improve antitumor responses.^{44–45} For higher affinity CARs, our data supports a clinical strategy of first evaluating the infusion of CAR-T without lymphodepletion and if safe, then

performing CAR T dose escalation with lymphodepletion. An alternative to avoid toxicity is locoregional delivery of CAR T without conditioning as has been used safely in patients with HER2+central nervous system (CNS) tumors.⁴⁶ Although not suitable to treat disseminated metastases, locoregional delivery to HER2+tumors may avoid infiltration into distal normal HER2+tissues. The question of whether locoregional delivery can effectively mitigate toxicity when targeting antigens other than HER2 remains an area requiring further investigation.

Our studies show that a therapeutic window for targeting HER2-high tumors is achievable with low-affinity CAR T or high-affinity CAR T that are constrained in antigen recognition due to scFv orientation. Safety thresholds for a given target and CAR will be difficult to predict and mitigation strategies that include titration of T-cell dose, lymphodepletion intensity, and logic-gating approaches^{44–45} should be considered in next-generation CAR design for targets such as HER2. High-throughput biophysical analysis of antibody binding and widespread availability of gene synthesis afford the rapid testing of new CAR designs and preclinical models can assist in defining principles to guide subsequent clinical evaluation.

Author affiliations

¹Immunotherapy Integrated Research Center, Fred Hutchinson Cancer Center, Seattle, Washington, USA

²Translational Science and Therapeutics Division, Fred Hutchinson Cancer Center, Seattle, Washington, USA

³Comparative Medicine, Fred Hutchinson Cancer Center, Seattle, Washington, USA

⁴Experimental Histopathology, Fred Hutchinson Cancer Center, Seattle, Washington, USA

⁵Molecular Design and Therapeutics, Fred Hutchinson Cancer Center, Seattle, Washington, USA

⁶Antibody Technology, Fred Hutchinson Cancer Center, Seattle, Washington, USA

Acknowledgements The authors thank Kimberly Smythe, Albert Yeh, and Andrew McGuire for valuable insights and supportive discussions. We thank Cyrus Ghajar for providing D2.0R tumor cells, Andrew McGuire for technical guidance with IgG sequencing methods, Andre Lieber for the sequence of 7.16.4 hybridoma, Richard Lawler for performing the Luminescence assay, Stephanie Weaver for help with IHC analysis, the staff of Antibody Technology, Experimental Histology, and Comparative Medicine, and Flow Cytometry Shared Resources for their technical support.

Contributors Guarantor (SRR); designing research studies (TBS, BGH, DJ, SRR); conducting experiments (TBS, ARS, SMS, KRS, BWS, EAG, JPP, DJ); acquiring data (TBS, ARS, SMS, KRS, BWS, EAG, ALK, DJ); analyzing data (TBS, ALK, DJ); providing reagents (JPP, JMO); writing the manuscript (TBS, SRR).

Funding This work was supported by funding from the NIH R01 CA114536 and P30 CA015704; the Department of Defense (DoD) W81XWH-20-0229 and W81XWH-22-0006; and Lyell Immunopharma SRA191207.

Competing interests SRR was a founder, has served as an advisor, and has patents licensed to Juno Therapeutics; is a founder of and holds equity in Lyell Immunopharma; and has served on the advisory boards for Adaptive Biotechnologies, Nohla and Ervaccine. The other authors have declared that no conflict of interest exists.

Patient consent for publication Not applicable.

Ethics approval Not applicable.

Provenance and peer review Not commissioned; externally peer reviewed.

Data availability statement Data are available upon reasonable request.

Supplemental material This content has been supplied by the author(s). It has not been vetted by BMJ Publishing Group Limited (BMJ) and may not have been peer-reviewed. Any opinions or recommendations discussed are solely those

of the author(s) and are not endorsed by BMJ. BMJ disclaims all liability and responsibility arising from any reliance placed on the content. Where the content includes any translated material, BMJ does not warrant the accuracy and reliability of the translations (including but not limited to local regulations, clinical guidelines, terminology, drug names and drug dosages), and is not responsible for any error and/or omissions arising from translation and adaptation or otherwise.

Open access This is an open access article distributed in accordance with the Creative Commons Attribution Non Commercial (CC BY-NC 4.0) license, which permits others to distribute, remix, adapt, build upon this work non-commercially, and license their derivative works on different terms, provided the original work is properly cited, appropriate credit is given, any changes made indicated, and the use is non-commercial. See <http://creativecommons.org/licenses/by-nc/4.0/>.

Author note Current address for Benjamin G Hoffstrom: UCLA Translational Oncology, 2825 Santa Monica Boulevard, Santa Monica, CA 90404. Bhoffstrom@mednet.ucla.edu

ORCID iDs

Tamer Basel Shabaneh <http://orcid.org/0000-0001-7895-7134>

Sylvain Simon <http://orcid.org/0000-0001-5985-3946>

REFERENCES

- Fesnak AD, June CH, Levine BL. Engineered T cells: the promise and challenges of cancer immunotherapy. *Nat Rev Cancer* 2016;16:566–81.
- June CH, Sadelain M. Chimeric antigen receptor therapy. *N Engl J Med* 2018;379:64–73.
- Cappell KM, Kochenderfer JN. Long-term outcomes following CAR T cell therapy: what we know so far. *Nat Rev Clin Oncol* 2023;20:359–71.
- Kampouri E, Walti CS, Gauthier J, et al. Managing hypogammaglobulinemia in patients treated with CAR-T-cell therapy: key points for clinicians. *Expert Rev Hematol* 2022;15:305–20.
- Newick K, O'Brien S, Moon E, et al. CAR T Cell therapy for solid tumors. *Annu Rev Med* 2017;68:139–52.
- Watanabe K, Kuramitsu S, Posey AD, et al. Expanding the therapeutic window for CAR T cell therapy in solid tumors: the knowns and unknowns of CAR T cell biology. *Front Immunol* 2018;9:2486.
- Wang E, Cesano A, Butterfield LH, et al. Improving the therapeutic index in adoptive cell therapy: key factors that impact efficacy. *J Immunother Cancer* 2020;8:e001619.
- Feng K-C, Guo Y-L, Liu Y, et al. Cocktail treatment with EGFR-specific and CD133-specific chimeric antigen receptor-modified T cells in a patient with advanced cholangiocarcinoma. *J Hematol Oncol* 2017;10:4.
- Guo Y, Feng K, Liu Y, et al. Phase I study of chimeric antigen receptor-modified T cells in patients with EGFR-positive advanced biliary tract cancers. *Clin Cancer Res* 2018;24:1277–86.
- Lamers CHJ, Klaver Y, Gratama JW, et al. Treatment of metastatic renal cell carcinoma (mRCC) with CAIX CAR-engineered T-cells—a completed study overview. *Biochem Soc Trans* 2016;44:951–9.
- Katz SC, Burga RA, McCormack E, et al. Phase I hepatic immunotherapy for metastases study of intra-arterial chimeric antigen receptor-modified T-cell therapy for CEA+ liver metastases. *Clin Cancer Res* 2015;21:3149–59.
- Zhang C, Wang Z, Yang Z, et al. Phase I escalating-dose trial of CAR-T therapy targeting CEA+ metastatic colorectal cancers. *Mol Ther* 2017;25:1248–58.
- Thistlethwaite FC, Gilham DE, Guest RD, et al. The clinical efficacy of first-generation carcinoembryonic antigen (CEACAM5)-specific CAR T cells is limited by poor persistence and transient pre-conditioning-dependent respiratory toxicity. *Cancer Immunol Immunother* 2017;66:1425–36.
- Haas AR, Golden RJ, Litzky LA, et al. Two cases of severe pulmonary toxicity from highly active mesothelin-directed CAR T cells. *Mol Ther* 2023;31:2309–25.
- Flugel CL, Majzner RG, Krenciute G, et al. Overcoming on-target, off-tumour toxicity of CAR T cell therapy for solid tumours. *Nat Rev Clin Oncol* 2023;20:49–62.
- Liu X, Zhang N, Shi H. Driving better and safer HER2-specific CARs for cancer therapy. *Oncotarget* 2017;8:62730–41.
- Wang DP, Fujii S, Konishi I, et al. Expression of c-erbB-2 protein and epidermal growth factor receptor in normal tissues of the female genital tract and in the placenta. *Virchows Arch A Pathol Anat Histopathol* 1992;420:385–93.
- Press MF, Cordon-Cardo C, Slamon DJ. Expression of the HER-2/neu proto-oncogene in normal human adult and fetal tissues. *Oncogene* 1990;5:953–62.
- Mazzotta M, Krasniqi E, Barchiesi G, et al. Long-term safety and real-world effectiveness of trastuzumab in breast cancer. *J Clin Med* 2019;8:254.
- Swain SM, Shastry M, Hamilton E. Targeting HER2-positive breast cancer: advances and future directions. *Nat Rev Drug Discov* 2023;22:101–26.
- Nie T, Blair HA. Trastuzumab deruxtecan: a review in unresectable or metastatic HER2-positive breast cancer. *Target Oncol* 2023;18:463–70.
- Xie YH, Chen YX, Fang JY. Comprehensive review of targeted therapy for colorectal cancer. *Signal Transduct Target Ther* 2020;5:22.
- Morgan RA, Yang JC, Kitano M, et al. Case report of a serious adverse event following the administration of T cells transduced with a chimeric antigen receptor recognizing ERBB2. *Mol Ther* 2010;18:843–51.
- Ahmed N, Brawley VS, Hegde M, et al. Human epidermal growth factor receptor 2 (HER2) -specific chimeric antigen receptor-modified T cells for the immunotherapy of HER2-positive sarcoma. *J Clin Oncol* 2015;33:1688–96.
- Hegde M, Joseph SK, Pashankar F, et al. Tumor response and endogenous immune reactivity after administration of HER2 CAR T cells in a child with metastatic rhabdomyosarcoma. *Nat Commun* 2020;11:3549.
- Feng K, Liu Y, Guo Y, et al. Phase I study of chimeric antigen receptor modified T cells in treating HER2-positive advanced biliary tract cancers and pancreatic cancers. *Protein Cell* 2018;9:838–47.
- Liu X, Jiang S, Fang C, et al. Affinity-tuned ErbB2 or EGFR chimeric antigen receptor T cells exhibit an increased therapeutic index against tumors in mice. *Cancer Res* 2015;75:3596–607.
- Castellarin M, Sands C, Da T, et al. A rational mouse model to detect on-target, off-tumor CAR T cell toxicity. *JCI Insight* 2020;5:e136012:14..
- Wang LXJ, Westwood JA, Moeller M, et al. Tumor ablation by gene-modified T cells in the absence of autoimmunity. *Cancer Res* 2010;70:9591–8.
- Hudecek M, Sommermeyer D, Kosasih PL, et al. The nonsignaling extracellular spacer domain of chimeric antigen receptors is decisive for in vivo antitumor activity. *Cancer Immunol Res* 2015;3:125–35.
- Chakraborty D, Ghosh S, Jain B, et al. Her2neu expression of gastric and lower esophageal carcinoma and its correlation with clinicopathological findings in tertiary care hospital in Eastern India. *Biomed Biotechnol Res J* 2022;6:203.
- Zhang Y, Li Y, Cao W, et al. Single-cell analysis of target antigens of CAR-T reveals a potential landscape of “on-target, off-tumor toxicity.” *Front Immunol* 2021;12:799206.
- Uhlén M, Fagerberg L, Hallström BM, et al. Proteomics. Tissue-based map of the human proteome. *Science* 2015;347:6220.
- Drebin JA, Stern DF, Link VC, et al. Monoclonal antibodies identify a cell-surface antigen associated with an activated cellular oncogene. *Nature* 1984;312:545–8.
- Seo H, Chen J, González-Avalos E, et al. TOX and TOX2 transcription factors cooperate with NR4A transcription factors to impose CD8+ T cell exhaustion. *Proc Natl Acad Sci U S A* 2019;116:12410–5.
- Zhang H, Wang Q, Montone KT, et al. Shared antigenic epitopes and pathobiological functions of anti-p185(her2/neu) monoclonal antibodies. *Exp Mol Pathol* 1999;67:15–25.
- Xiao Q, Zhang X, Tu L, et al. Size-dependent activation of CAR-T cells. *Sci Immunol* 2022;7:eabl3995.
- Chmielewski M, Hombach A, Heuser C, et al. T cell activation by antibody-like immunoreceptors: increase in affinity of the single-chain fragment domain above threshold does not increase T cell activation against antigen-positive target cells but decreases selectivity. *J Immunol* 2004;173:7647–53.
- Muranski P, Boni A, Wrzesinski C, et al. Increased intensity lymphodepletion and adoptive immunotherapy—how far can we go? *Nat Clin Pract Oncol* 2006;3:668–81.
- Gattinoni L, Finkelstein SE, Klebanoff CA, et al. Removal of homeostatic cytokine sinks by lymphodepletion enhances the efficacy of adoptively transferred tumor-specific CD8+ T cells. *J Exp Med* 2005;202:907–12.
- Dudley ME, Yang JC, Sherry R, et al. Adoptive cell therapy for patients with metastatic melanoma: evaluation of intensive myeloablative chemoradiation preparative regimens. *J Clin Oncol* 2008;26:5233–9.
- Onsum MD, Geretti E, Paragas V, et al. Single-cell quantitative HER2 measurement identifies heterogeneity and distinct subgroups

- within traditionally defined HER2-positive patients. *Am J Pathol* 2013;183:1446–60.
- 43 McLane LM, Abdel-Hakeem MS, Wherry EJ. CD8 T cell exhaustion during chronic viral infection and cancer. *Annu Rev Immunol* 2019;37:457–95.
 - 44 Srivastava S, Salter AI, Liggitt D, *et al.* Logic-gated ROR1 chimeric antigen receptor expression rescues T cell-mediated toxicity to normal tissues and enables selective tumor targeting. *Cancer Cell* 2019;35:489–503.
 - 45 Tousley AM, Rotiroti MC, Labanieh L, *et al.* Co-opting signalling molecules enables logic-gated control of CAR T cells. *Nature* 2023;615:507–16.
 - 46 Vitanza NA, Johnson AJ, Wilson AL, *et al.* Locoregional infusion of HER2-specific CAR T cells in children and young adults with recurrent or refractory CNS tumors: an interim analysis. *Nat Med* 2021;27:1544–52.
 - 47 Cho H-S, Mason K, Ramyar KX, *et al.* Structure of the extracellular region of HER2 alone and in complex with the herceptin fab. *Nature* 2003;421:756–60.